Electron-hole collision limited resistance of gapped graphene

Arseny Gribachov◉ and Dmitry Svintsov◉*

Moscow Institute of Physics and Technology, 141700 Dolgoprudny, Russia

Vladimir Vyurkov◉

Moscow Institute of Physics and Technology, 141700 Dolgoprudny, Russia
and Valiev Institute of Physics and Technology RAS, 36/1 Nahimovsky Ave., 117218 Moscow, Russia

Collisions between electrons and holes can dominate the carrier scattering in clean graphene samples in the vicinity of the charge neutrality point. While electron-hole limited resistance in pristine gapless graphene is well studied, its evolution with induction of band gap E_g is less explored. Here, we derive the functional dependence of electron-hole collision limited resistance of gapped graphene ρ_{eh} on the ratio of gap and thermal energy E_g/kT. At low temperatures and large band gaps, the resistance grows linearly with E_g/kT and possesses a minimum at $E_g \approx 2.5kT$. This contrasts to the Arrhenius activation-type behavior for intrinsic semiconductors. Introduction of impurities restores the Arrhenius law for resistivity at low temperatures and/or high doping densities. The hallmark of electron-hole collision effects in graphene resistivity at charge neutrality is thus the crossover between exponential and power-law resistivity scalings with temperature.

I. INTRODUCTION

The problem of minimal dc graphene conductivity $\sigma_{\min}$ observed at charge neutrality has been a subject of long debate since the discovery of graphene. Experimental studies have shown that $\sigma_{\min}$ varies slightly between samples and with changing the temperature [1–3], which posed questions about the universality of this quantity. Numerous theoretical works attempted to derive $\sigma_{\min}$ from Kubo's formula for clean graphene at zero frequency of electric field ω, zero temperature T, and doping ε_F [4–6]. The apparent "universal" result appeared to depend on the order of taking the limits of zero frequency, temperature, and doping [7]. The latter fact is indicated on the deficiency of the "clean graphene" model for the derivation of universal minimal conductivity.

The first resolution of the minimal conductivity puzzle appeared by realizing that graphene at charge neutrality has some residual doping. This doping comes from random impurities in the sample, arranged in positively and negatively charged clusters. The free carriers tend to screen these impurity charges, forming the electron-hole puddles [8]. The root-mean-square density of charge carriers appears to be nonzero. Instead, it is proportional to the impurity density n_i and so is the carrier scattering rate. These two proportionalities lead to a very weak dependence of $\sigma_{\min}$ on the density of residual impurities and temperature, which can be considered as "approximate universality" [9,10].

With the current level of graphene technology, the density of residual impurities can readily be lower than the density of thermally activated electrons and holes $n_{\mathrm{th}} \approx 8 \times 10^{10}$ cm^{-2}

[11]. In such a situation, electron-hole puddles and impurity scattering make a minor contribution to the resistivity. The scattering between electrons and holes (e-h scattering) now governs the experimentally measured value of minimum conductivity [12–15]. A strong violation of the Wiedemann-Frantz relation between electrical and thermal conductivity at charge neutrality [16] and the appearance of new electron-hole sound waves [17] also indicate the dominant role of e-h scattering in clean samples. A scaling estimate of e-h limited conductivity was presented in Ref. [18] and resulted in $\sigma_{\min} = C\alpha_c^{-2}e^2/h$, where $\alpha_c = e^2/\hbar v_0$ is the Coulomb coupling constant, v_0 is the velocity of massless electrons in graphene, and C is the numerical prefactor. A rigorous solution of the kinetic equation using the variational principle confirmed the result and established $C \approx 0.76$ [19,20].

While most theoretical and experimental studies were devoted to the electron-hole scattering in pristine gapless graphene, little attention has been paid to the same process in gapped systems. The gap induction in a single graphene layer is possible under lattice reconstruction on boron nitride substrates [21]. The gap is readily induced in a graphene bilayer under the action of transverse electric field [22,23]. The derivatives of graphene are not the only examples of two-dimensional (2D) electron systems with small energy gap. Another family is represented by quantum wells based on mercury cadmium telluride of subcritical thickness [24,25]. Given the large variety of clean 2D systems with small band gap and their potential applications in nano- and optoelectronics, it is natural to study the factors limiting their electrical resistivity, particularly, the inevitable electron-hole scattering. In Ref. [26] it was suggested that e-h scattering time weakly depends on the induced gap in such systems. An attempt to evaluate and measure the electron-hole limited resistivity was

*svintcov.da@mipt.ru

presented in [27]. These results cannot be considered as satisfactory because the e-h scattering times τ_{eh} in the presence of band gap E_g were not derived, but rather suggested. The authors of [27] have proposed a universal function $f(E_g/kT)$ governing the scaling of e-h limited conductivity with band gap; the function possessed a quadratic maximum at $E_g = 0$ and dropped exponentially at $E_g/kT \gg 1$. Such dependence was seemingly confirmed by the experiment.

The present paper is aimed at a rigorous derivation of electron-hole scattering time and conductivity at the neutrality point in gapped graphene. Our formalism is based on a kinetic equation with carrier-carrier collision integral; the carriers are assumed interacting via unscreened Coulomb potential. We find that, at large band gaps, the conductivity scales as $\sigma_{\min} \propto kT/E_g$. This behavior differs essentially from conventional Arrhenius-type activation.

The non-Arrhenius behavior of minimal conductivity can be explained with simple gas kinetics arguments. The free path time of a trial electron against a dilute hole background is inversely proportional to the hole density $\tau_{eh} \propto n_h^{-1} \propto e^{E_g/2kT}$, i.e., grows exponentially with gap induction. The Drude conductivity is proportional to the product of electron density and free-path time, $\sigma_{\min} \propto n_e \tau_{eh}/m^*$. As electron and hole components are balanced at charge neutrality, $n_e = n_h$, the leading Arrhenius exponents are canceled in the expression for conductivity. Eventually, the conductivity depends on the gap only via effective mass, $m^* = E_g/2v_0^2$. This justifies the hyperbolic dependence of $\sigma_{\min}$ on E_g.

The above intuitive explanation is missing the long-range character of Coulomb interaction. In classical plasmas, the latter led to a log-divergent collision integral [28]. We show that no such divergences appear during the evaluation of conductivity. The collision integral converges both at small momentum transfers $q \to 0$ as such momenta do not change the electric current and at large momenta $q \to \infty$ due to small quantum-mechanical overlap between scattered states. All in all, our variational derivation results in the following expression for the conductivity at charge neutrality valid at $E_g \gg kT$:

$$\sigma_{\min} = \frac{8}{\pi} \frac{e^2}{h} \alpha_C^{-2} \frac{kT}{E_g}. \tag{1}$$

II. VARIATIONAL APPROACH TO KINETIC EQUATION WITH CARRIER-CARRIER COLLISIONS

Electron states in the gapped graphene are described by a "massive" Dirac Hamiltonian

$$\hat{\mathcal{H}}_D = \begin{bmatrix} E_g/2 & v_0(\hat{p}_x - i\hat{p}_y) \\ v_0(\hat{p}_x + i\hat{p}_y) & -E_g/2 \end{bmatrix}.$$

Such Hamiltonian is applicable to the single layer graphene aligned to a boron nitride substrate and to a 2D electron system in CdHgTe quantum wells. Its applicability to graphene bilayer is limited, as the latter has a quadratic band touching at $E_g = 0$. In Sec. V we will discuss which of our results are independent of the particular structure of the low-energy Hamiltonian.

The dc conductivity is obtained by solving the kinetic equation with respect to distribution function, which we
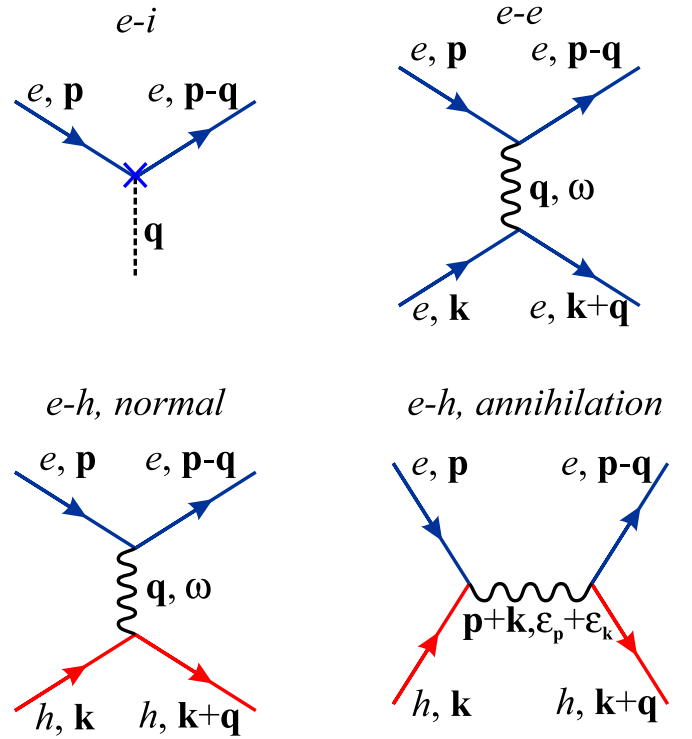

FIG. 1. Scattering diagrams for the processes contributing to graphene resistivity at the charge neutrality point: electron-impurity, electron-electron, and electron-hole scattering (normal and annihilation-type processes).

linearize as $f_p = f_0 - \Phi_{e/h,\mathbf{p}} \partial f_0/\partial \varepsilon$; here $\Phi_{e/h,\mathbf{p}}$ is the linear function of electric field $\mathbf{E}$ and the subscripts e and h distinguish between electrons and holes. We restrict our consideration to the carrier-carrier and carrier-impurity collisions. The former involve electron-electron (e-e), hole-hole (h-h), and electron-hole (e-h) collisions (Fig. 1). The kinetic equation for electrons takes on the form

$$-e(\mathbf{E} \cdot \mathbf{v_p})\frac{\partial f_0}{\partial \varepsilon} = -\mathcal{C}_{ei}\{\Phi_{e,\mathbf{p}}\} - \mathcal{C}_{ee}\{\Phi_{e,\mathbf{p}}\} - \mathcal{C}_{eh}\{\Phi_{e,\mathbf{p}}, \Phi_{h,\mathbf{p}}\}$$

$$\tag{2}$$

and similarly for holes with apparent change of signs. At charge neutrality electrons and holes move in the opposite directions; thus $\Phi_{e,\mathbf{p}} = -\Phi_{h,\mathbf{p}} \equiv \Phi_{\mathbf{p}}$. The complex structure of carrier-carrier collision integrals makes the exact solution of (2) impossible, at least in the nondegenerate case [29]. For this reason, we use the variational approach with a reasonable trial form of distribution function to get an estimate of the resistivity [30,31]. The problem of resistivity is weakly sensitive to the specific form of $\Phi_{\mathbf{p}}$ (unlike the problems of thermoelectric coefficients [32]); thus the variational approach is efficient for predicting its functional dependence.

Within this approach, the kinetic equation being the linear integral equation with respect to $\Phi_{\mathbf{p}}$ is considered as an extremum condition of a functional $\mathcal{Q}[\Phi]$ being quadratic in $\Phi_{\mathbf{p}}$. The procedure of generating $\mathcal{Q}[\Phi]$ from a linear equation (2) is inverse to obtaining an Euler-Lagrange equation from a

given functional in variational calculus. Proceeding this way, we find an explicit form of $\mathcal{Q}[\Phi]$ [33]:

$$\mathcal{Q}[\Phi] = \mathcal{Q}_{ei}[\Phi] + \mathcal{Q}_{ee}[\Phi] + \mathcal{Q}_{eh}[\Phi] - \mathcal{Q}_{\text{field}}[\Phi], \quad (3)$$

$$\mathcal{Q}_{\text{field}}[\Phi] = -eN \sum_{\mathbf{p}} (\mathbf{v_p} \cdot \mathbf{E}) \frac{\partial f_0}{\partial \varepsilon} \Phi_{\mathbf{p}}, \quad (4)$$

$$\mathcal{Q}_{ei}[\Phi] = \frac{N}{2} \sum_{\mathbf{pp'}} \frac{\partial f_0}{\partial \varepsilon} (\Phi_p - \Phi_{p'})^2 W^{ei}_{\mathbf{pp'}}, \quad (5)$$

$$\mathcal{Q}_{ee}[\Phi] = \frac{N}{8} \frac{1}{kT} \sum_{\mathbf{pkq}} f_0(\mathbf{p}) f_0(\mathbf{k})[1 - f_0(\mathbf{p'})][1 - f_0(\mathbf{k'})]$$
$$\times W^{ee}_{\mathbf{pk,p'k'}} [(\Phi_p + \Phi_k) - (\Phi_{p'} + \Phi_{k'})]^2, \quad (6)$$

$$\mathcal{Q}_{eh}[\Phi] = \frac{N}{8} \frac{1}{kT} \sum_{\mathbf{pkq}} f_0(\mathbf{p}) f_0(\mathbf{k})[1 - f_0(\mathbf{p'})][1 - f_0(\mathbf{k'})]$$
$$\times W^{eh}_{\mathbf{pk,p'k'}} [(\Phi_p - \Phi_k) - (\Phi_{p'} - \Phi_{k'})]^2. \quad (7)$$

Above, W^{ei}, W^{ee}, and W^{eh} are the Fermi golden rule scattering probabilities of electron-impurity, electron-electron, and electron-hole collisions. The corresponding scattering diagrams are shown in Fig. 1. Recalling the large spin-valley degeneracy factor for graphene $N = 4$, we neglect the exchange scattering for electron-electron collisions; the latter is possible if only both electrons have the same spin and belong to the same valley. For electron-hole collisions, the exchange (or annihilation) scattering cannot be neglected. An electron and a hole undergoing an annihilation process should still have the same spin and valley, yet the emanating virtual photon can produce the final-state pair with any spin in any valley. This results in equal orders of magnitude for normal and annihilation e-h scattering even in the large-N limit. With these prerequisites, we adopt the scattering probabilities in the form

$$W^{ei}_{\mathbf{pp'}} = \frac{2\pi}{\hbar} n_{\text{imp}} |V(\mathbf{q})|^2 |M^{++}_{\mathbf{pp'}}|^2 \delta(\varepsilon_{\mathbf{p}} - \varepsilon_{\mathbf{p'}}), \quad (8)$$

$$W^{ee}_{\mathbf{pk,p'k'}} = \frac{2\pi}{\hbar} N |V(\mathbf{q})|^2 |M^{++}_{\mathbf{pp'}}|^2 |M^{++}_{\mathbf{kk'}}|^2 \delta(\varepsilon_{\mathbf{p}} + \varepsilon_{\mathbf{k}} - \varepsilon_{\mathbf{p'}} - \varepsilon_{\mathbf{k'}}), \quad (9)$$

$$W^{eh}_{\mathbf{pk,p'k'}} = \frac{2\pi}{\hbar} N [|V(\mathbf{q})|^2 |M^{--}_{\mathbf{pp'}}|^2 |M^{++}_{\mathbf{kk'}}|^2 + |V(\mathbf{p} + \mathbf{k})|^2$$
$$\times |M^{+-}_{\mathbf{pk}}|^2 |M^{+-}_{\mathbf{p'k'}}|^2] \delta(\varepsilon_{\mathbf{p}} + \varepsilon_{\mathbf{k}} - \varepsilon_{\mathbf{p'}} - \varepsilon_{\mathbf{k'}}), \quad (10)$$

where $N = 4$ is the degeneracy factor, $\varepsilon_p = (E_g^2/4 + p^2 v_0^2)^{1/2}$ is the energy spectrum in the gapped graphene, $V(\mathbf{q}) = 2\pi e^2/\kappa |\mathbf{q}|$ is the Fourier-transformed Coulomb potential, κ is the background dielectric constant, and $M^{ss'}_{\mathbf{pp'}}$ is the overlap of chiral wave functions between bands s and s' ($s = +1$ for the conduction and $s = -1$ for the valence band, respectively):

$$|M^{ss'}_{\mathbf{pp'}}|^2 = \frac{\varepsilon_p \varepsilon_{p'} + (E_g/2)^2 + ss'(v_0 \mathbf{p} \cdot v_0 \mathbf{p'})}{2\varepsilon_p \varepsilon_{p'}}. \quad (11)$$

A fundamental difference between effects of e-e and e-h collision integrals should be mentioned at that stage. There is a difference in signs with which the function $\Phi_{\mathbf{p}}$ enters the expressions (6) and (7). It stems from the fact that $\mathcal{Q}[\Phi]$ is

sensitive only to the collisions changing the electric current; the quadratic-in-Φ expression in square brackets of (6) and (7) are proportional to this change. Naturally, the current carried by two particles with momenta $\mathbf{p}$ and $\mathbf{k}$ depends on their charge, which explains the difference of collision integrals for e-e and e-h scattering.

Our trial distribution function is selected as

$$\Phi_{\mathbf{p}} = \tau \, e(\mathbf{v_p} \cdot \mathbf{E}), \quad (12)$$

where τ is the parameter subjected to the optimization having the meaning of transport relaxation time and $\mathbf{v_p} = \partial \varepsilon_{\mathbf{p}}/\partial \mathbf{p}$ is the electron velocity. The angular dependence of $\Phi_{\mathbf{p}} \propto \cos \theta_{\mathbf{p}}$ is dictated by the angular dependence of the driving term in kinetic equation $(\mathbf{E} \cdot \mathbf{v_p}) \propto \cos \theta_{\mathbf{p}}$. The dependence on absolute value of momentum $\Phi_{\mathbf{p}} \propto v_p$ is important to reproduce the finite resistivity of gapless graphene. Other forms lead to the log-divergent collision integral due to the prolonged interaction of carriers with collinear momenta [20]. In the gapped case, $\Phi_{\mathbf{p}}$ given by (12) is not the only possible choice, but we stick to it for traceability of our result to the preceding studies.

The optimization of the functional $\mathcal{Q}[\Phi]$ with respect to the scattering time yields the following result:

$$\tau = \frac{D}{C}, \quad \sigma = D\tau, \quad (13)$$

where D is the Drude weight and $C = C_{ei} + C_{ee} + C_{eh}$ is the net collision rate. The Drude weight is given by a conventional expression,

$$D = -\frac{N e^2}{2} \sum_{\mathbf{p}} v_p^2 \frac{\partial f_0}{\partial \varepsilon}, \quad (14)$$

which has the following asymptotics:

$$D = \frac{N e^2 kT}{4\pi \hbar^2} \begin{cases} \ln 2 + \left(\ln 2 - \frac{1}{8}\right)\left(\frac{E_g}{2kT}\right)^2, & E_g \ll kT, \\ 2\frac{E_g/kT - 2}{E_g/kT} \exp\left(-\frac{E_g}{2kT}\right), & E_g \gg kT. \end{cases} \quad (15)$$

The scattering rates C_{ei}, C_{ee}, and C_{eh} are the statistically averaged collision probabilities:

$$C_{ei} = \frac{N e^2}{2} \sum_{\mathbf{pp'}} \frac{\partial f_0}{\partial \varepsilon} (\mathbf{v_p} - \mathbf{v_{p'}})^2 W^{ei}_{\mathbf{pp'}}, \quad (16)$$

$$C_{ee} = \frac{N e^2}{8kT} \sum_{\mathbf{pkq}} f_0(\mathbf{p}) f_0(\mathbf{k})[1 - f_0(\mathbf{p'})][1 - f_0(\mathbf{k'})]$$
$$\times W^{ee}_{\mathbf{pk,p'k'}} [(\mathbf{v_p} + \mathbf{v_k}) - (\mathbf{v_{p'}} + \mathbf{v_{k'}})]^2, \quad (17)$$

$$C_{eh} = \frac{N e^2}{8kT} \sum_{\mathbf{pkq}} f_0(\mathbf{p}) f_0(\mathbf{k})[1 - f_0(\mathbf{p'})][1 - f_0(\mathbf{k'})]$$
$$\times W^{eh}_{\mathbf{pk,p'k'}} [(\mathbf{v_p} - \mathbf{v_k}) - (\mathbf{v_{p'}} - \mathbf{v_{k'}})]^2. \quad (18)$$

Expressions for the e-e and e-h collision rates look very similar and seem formally of the same order of magnitude. However, in the parabolic gap case (realized at $E_g \gg kT$), the momentum conservation upon e-e collisions implies the conservation of total current by the virtue of proportionality $\mathbf{p} = m^* \mathbf{v_p}$. This feature is captured by Eq. (17), where the velocity factor in the square brackets is exactly zero if

$\mathbf{p} = m^* \mathbf{v_p}$. Even in the gapless case, where proportionality between velocity and momentum does not hold, e-e collisions make a *numerically small* contribution to resistivity, compared to the e-h processes [23,34].

Expressions (13)–(18) are the central results of our paper and enable the direct evaluation of conductivity for the arbitrary value of the gap. One can resolve the delta-functional energy constraint in Eqs. (17) and (18) analytically (Appendix A) and proceed with the remaining four-dimensional integral numerically. A fully analytical expression for electron-hole scattering-limited resistivity can be obtained in the limit of large gaps $E_g \gg kT$, as described in Appendix B.

III. GAP-DEPENDENT CONDUCTIVITY LIMITED BY CARRIER-CARRIER SCATTERING

We start our inspection of collision frequencies τ^{-1} and resistivity $\rho = \sigma^{-1}$ from the case of pristine graphene, i.e., neglecting the electron-impurity collisions. Such a problem has only two dimensionless parameters: the coupling constant $\alpha_c = e^2/\kappa\hbar v_0$ and the normalized gap E_g/kT. Within the Born approximation to carrier-carrier scattering, the collision frequency and resistivity appear proportional to the coupling constant squared. Restoring the dimensionality of the collision rate and resistivity, we are always able to present them in the form

$$\tau_{eh}^{-1} = \alpha_c^2 \frac{kT}{\hbar} \tilde{\nu}\left(\frac{E_g}{kT}\right), \tag{19}$$

$$\sigma_{eh} = \frac{e^2}{\hbar} \alpha_c^{-2} \tilde{\sigma}\left(\frac{E_g}{kT}\right), \tag{20}$$

where $\tilde{\nu}$ and $\tilde{\sigma}$ are the dimensionless collision frequency and the dimensionless conductivity depending only on the normalized gap E_g/kT.

The resulting dependences of scattering rate and resistivity on E_g/kT are shown in Fig. 2. The collision frequency $\tilde{\nu}$ decays monotonically with increasing the gap, which reflects the lack of thermally excited carriers to collide within a nondegenerate semiconductor. It is possible to show that $\tilde{\nu} \propto e^{-E_g/2kT}$ at $E_g/kT \gg 1$. Still, the conductivity $\tilde{\sigma}_{eh}$ is scaling with the gap nonexponentially. The reason is that Drude weight D has a compensating exponential $D \propto e^{-E_g/2kT}$, which again reflects the exponentially small number of carriers in the band. The resulting dependence of $\tilde{\sigma}_{eh}$ on E_g/kT appears to be hyperbolic at large values of the gap, while the resistivity scales linearly, $\rho_{eh} \propto E_g/kT$. The latter scaling can be ascribed to the enhancement of effective mass in the Drude formula $\sigma_{eh} = ne^2\tau_{eh}/m^*$, provided the combination $n\tau_{eh}$ is gap independent.

Analyzing the intermediate-gap region, $E_g \sim kT$, it is instructive to split the electron-hole collision frequency into the contributions of "normal" and "annihilation-type" scattering. The dependences of partial collision frequencies on E_g/kT are both decaying, yet the annihilation collision frequency decays faster than the normal collision frequency. This fact is explained by approximate orthogonality of conduction and valence band states located in the kT window near the edges of conduction and valence bands. It is the states orthogonality which reduces the probability of annihilation, $|M_{\mathbf{pk}}^{+-}|^2 \ll 1$,
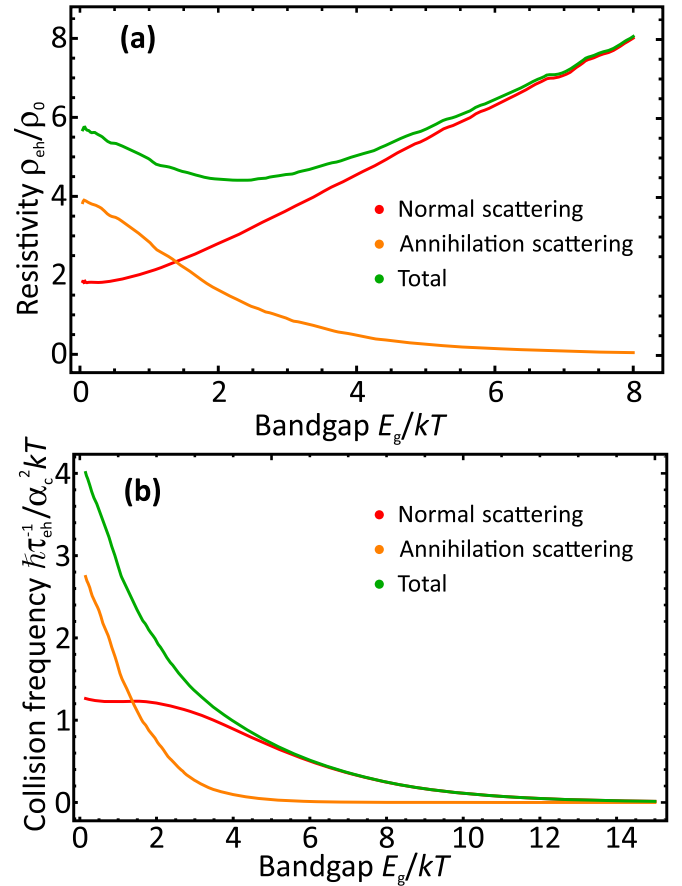

FIG. 2. Electron-hole limited resistivity ρ_{eh} (a) and associated collision frequency τ_{eh} (b) of pristine gapped graphene at the charge neutrality point. The collision frequency is scaled by "thermal frequency" $\alpha_c^2 kT/\hbar$, while the resistivity is scaled by $\rho_0 = \alpha_c^2 h/2e^2$. The partial contributions of normal and annihilation-type electron-hole scattering are shown with red and orange curves, respectively.

and makes the annihilation-type collisions irrelevant to the conductivity of the large-gap semiconductor. Yet, the annihilation scattering is large in the zero-gap state, even stronger than the conventional scattering.

Large frequency of annihilation-type collisions at $E_g = 0$ and its rapid decay at $E_g \gg kT$ result in a nontrivial dependence of resistivity on band gap E_g/kT. At small induced gaps, the resistivity decays due to the rapid cancellation of annihilation-type scattering and reaches a minimum at $E_g \approx 2.5kT$. At larger values of E_g, the resistivity grows linearly due to the enhancement of effective mass. The presence of such *annihilation minimum* on the gap dependence of resistance is a natural hallmark of the carrier-carrier collision limited transport.

To conclude the study of resistivity in pristine gapped graphene, we point to the main steps in deriving an approximate expression for resistivity at large band gaps. In that case, exchange electron-hole and electron-electron contributions to C can be neglected. The Fermi distribution functions are reduced to the Boltzmann exponents, which simplifies the energy integration. The natural cutoff for the transferred momentum q appears order of E_g/v_0—otherwise, the scattered

electron cannot reside on the dispersion curve. The latter fact disables the appearance of the Coulomb logarithm [28] in the expression for resistivity. Performing these steps, described in detail in Appendix B, we arrive at the conductivity of graphene with large induced gap in the form

$$\sigma_{eh}(E_g \gg kT) = \frac{8}{\pi} \frac{e^2}{h} \alpha_c^{-2} \frac{kT}{E_g}. \tag{21}$$

This value is very different numerically from the e-h limited conductivity of gapless graphene, obtained in Ref. [20] and reproduced in our calculations:

$$\sigma_{eh}(E_g = 0) = 0.76 \frac{e^2}{h} \alpha_c^{-2}. \tag{22}$$

Despite numerical and functional differences between small- and large-gap asymptotics of σ_{eh}, both (21) and (22) can be presented in a similar form. This is achieved by introducing the "running" coupling constant depending on the average thermal carrier velocity $\langle v_p^2 \rangle$

$$\overline{\alpha}_c^2 = \frac{e^4}{\kappa^2 \hbar^2 \langle v_p^2 \rangle}. \tag{23}$$

Here $\langle v_p^2 \rangle = v_0^2$ in the gapless state ($\overline{\alpha}_c \to \alpha_c$) and $\langle v_p^2 \rangle = 2kT/m^*$ in the limit of the large gap. With the notation (23), we present the large-gap conductivity as

$$\sigma_{eh}(E_g \gg kT) = \frac{2}{\pi} \frac{e^2}{h} \overline{\alpha}_c^{-2} \approx 0.6 \frac{e^2}{h} \overline{\alpha}_c^{-2}. \tag{24}$$

We may now speculate that the gap-dependent electron-hole collision limited conductivity of the variable-gap semiconductor is more universal than it was assumed previously [27]. First, the scaling of σ_{eh} with the gap is nonexponential and much slower. Second, the conductivity can be expressed only via conductance quantum e^2/h and the running coupling constant $\overline{\alpha}_c$, with a numerical prefactor very weakly depending on the gap.

IV. OBSERVABILITY OF THE ELECTRON-HOLE CONDUCTIVITY IN DISORDERED SAMPLES

It is now tempting to compare the magnitudes of the carrier-carrier and carrier-impurity contributions to the resistivity in realistic disordered samples. Within the adopted variational approach, the contributions of these scattering channels to the collision frequency and resistivity are additive:

$$\frac{1}{\tau} = \frac{1}{\tau_{eh}} + \frac{1}{\tau_{ei}}, \tag{25}$$

$$\rho = \rho_{eh} + \rho_{ei}. \tag{26}$$

From scaling considerations, the e-i collision frequency should be of the form

$$\tau_{ei}^{-1} = \alpha_c^2 \frac{n_{\text{imp}}}{(kT/\hbar v_0)^2} \frac{kT}{\hbar} \tilde{v}_{ei}\left(\frac{E_g}{kT}\right). \tag{27}$$

The normalized electron-impurity collision frequency $\tilde{v}_{ei}$ depends weakly on the scaled band gap E_g/kT and tends to
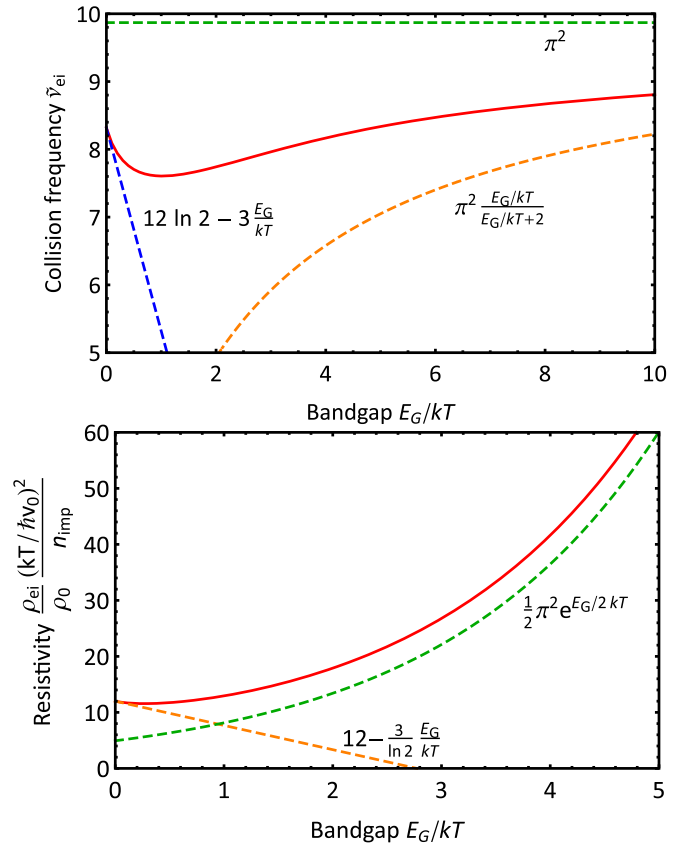

FIG. 3. Dependence of normalized electron-impurity collision frequency $\tilde{v}_{ei}$ (a) and resistivity ρ_{ei} (b) on the band gap scaled by temperature E_G/kT. Solid lines show the result of full variational calculation; dashed lines stand for small-gap and large-gap asymptotics, Eqs. (28) and (29).

constant values both in the limits $E_g \to 0$ and $E_g \gg kT$:

$$\tilde{v}_{ei} \approx \begin{cases} 12 \ln 2 - 3\frac{E_G}{kT}, & E_G \ll kT, \\ \pi^2 \frac{E_G/kT}{2 + E_G/kT}, & E_G \gg kT. \end{cases} \tag{28}$$

The resistivity limited by e-i collisions interpolates between a constant at zero gap and Arrhenius-type activation at large gap:

$$\rho_{ei} = \rho_0 \frac{(kT/\hbar v_0)^2}{n_{\text{imp}}} \begin{cases} 12 - \frac{3}{\ln 2} \frac{E_G}{kT}, & E_G \ll kT, \\ \frac{\pi^2}{2} \exp\left(\frac{E_G}{2kT}\right), & E_G \gg kT, \end{cases} \tag{29}$$

where we have introduced the "universal resistivity" $\rho_0 = \alpha_c^2 h / 2e^2$. The full dependence of electron-impurity collision frequency and resistivity along with their asymptotic values (28) and (29) are shown in Fig. 3.

It becomes clear now that the e-h scattering-limited resistivity is dominant over impurity-limited if the hole density exceeds the impurity density. With increasing the band gap, the number of thermally excited carriers is reduced, while the density of impurities remains approximately constant. This makes us conclude that e-h collisions always become weak at $E_g/kT \gg 1$.

The latter conclusion is illustrated in Fig. 4, where the total resistivity is shown as a function of inverse temperature at various impurity densities and band gaps. At the smallest band
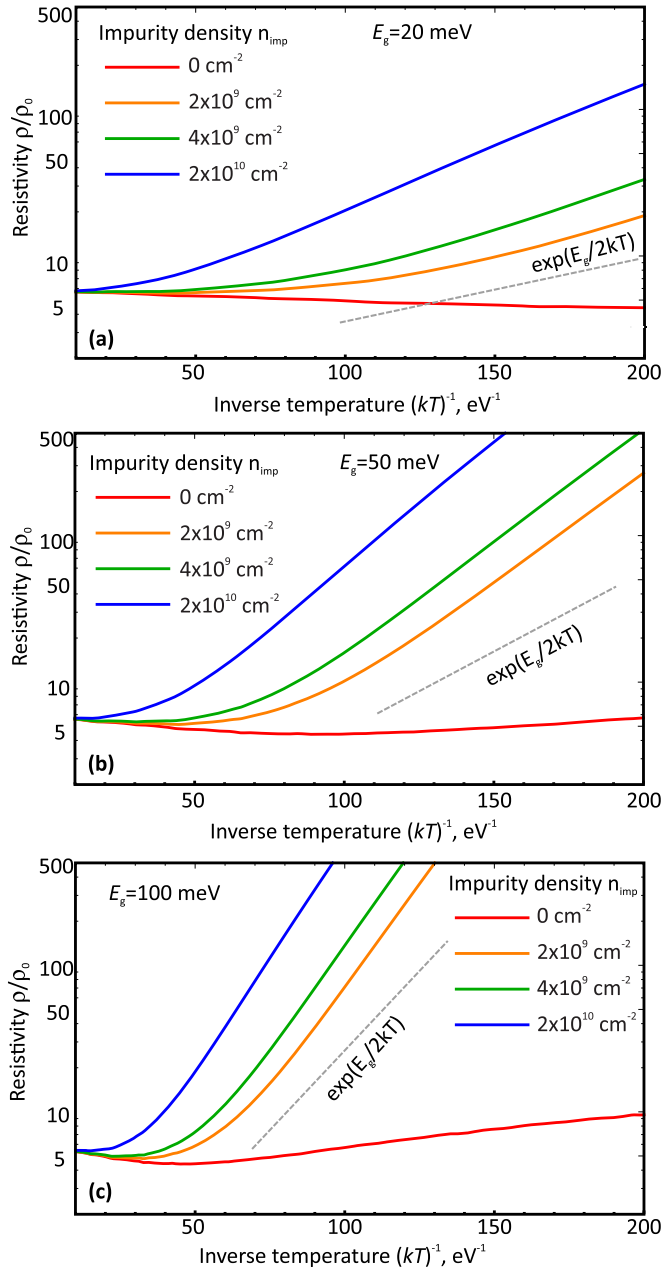
FIG. 4. Temperature-dependent resistivity ρ of gapped graphene under the combined action of electron-hole and impurity scattering for various values of band gap: $E_g = 20$ meV (a), $E_g = 50$ meV (b), and $E_g = 100$ meV (c). The resistivity is scaled by $\rho_0 = \alpha_c^2 h / 2e^2$. Curves of different colors correspond to different impurity densities n_{imp}: red curve in each panel corresponds to the pristine graphene; gray dashed line is a guide for the eye showing the Arrhenius behavior.

gap $E_g = 20$ meV [Fig. 4(a)], the total resistivity is dominated by e-h collisions in a wide temperature range starting from the highest temperatures to $(kT)^{-1} \approx 60$ eV^{-1} ($T \approx 200$ K). With increasing the band gap to $E_g = 50$ meV and then to $E_g = 100$ meV [Figs. 4(b) and 4(c)], we observe quite a rapid increase in total resistivity. The total resistivity deviates from the electron-hole limited one already at nearly room temperature and becomes dominated by impurities. The Arrhenius law

for impurity scattering is expectantly fulfilled: the logarithm of resistivity vs T^{-1} becomes linear (see the gray dashed curve in Fig. 4). We suggest that the seeming agreement between the exponential e-h conductivity scaling function $f(E_g/kT)$ of Ref. [27] and experiment was due to the presence of residual impurities, which guaranteed the restoration of Arrhenius law.

The density of impurities in gapped graphene should be pretty low to observe the effects of electron-hole scattering below the room temperature. For $E_g = 20$ meV and $n_{imp} = 2 \times 10^9$ cm^{-2}, the e-h and e-i contributions to resistivity become equal to each other at $T \approx 90$ K. Such density of impurities is achievable in high-quality van der Waals heterostructures.

V. DISCUSSION AND CONCLUSIONS

We have performed a systematic variational evaluation of resistivity due to electron-hole and electron-impurity scattering in gapped graphene. We have found that, for pristine graphene, the resistivity at the charge neutrality point scales as $\rho_{eh} \propto E_g/kT$. The scaling is nonexponential and violates the empirical Arrhenius law. This fact is related to simultaneous reduction in carrier density and collision frequency with increasing the band gap. A weak residual dependence of resistivity on the gap is due to the gap-dependent effective mass within the Dirac model.

Another important feature of gap-dependent resistivity $\rho_{eh}(E_g/kT)$ is the presence of minimum achieved at $E_g \approx 2.5kT$. This minimum is provided by the competition of two opposite effects occurring upon gap induction: the enhancement of effective mass and reduction in probability of electron-hole annihilation scattering. Such an *annihilation minimum* is quite sensitive to the numerical values of the normal and annihilation scattering probabilities. Rigorously speaking, the minimum may not appear for other model potentials of electron-hole scattering, e.g., statically screened or dynamically screened Coulomb interaction. Still, the effects of screening should be small in the gapped case $E_g/kT \gg 1$, where the number of free carriers is low.

Our consideration was limited here to carrier-carrier and carrier-impurity scattering. At elevated temperatures, the carrier-phonon scattering can become dominant. Inclusion of acoustic phonon scattering is achieved similarly to carrier-impurity scattering, Eq. (5), with the scattering probability replaced with

$$W_{\mathbf{pp}'}^{e-ph} = \frac{2\pi}{\hbar} \frac{T}{\hbar \omega_q} \mathcal{D}^2 \frac{q^2 \hbar}{\rho \omega_q} |M_{\mathbf{pp}'}^{++}|^2 \delta(\varepsilon_{\mathbf{p}} - \varepsilon_{\mathbf{p}'}), \qquad (30)$$

where $\mathcal{D} \sim 10$ eV is the deformation potential constant, ρ is the sheet density of graphene, $\mathbf{q} = \mathbf{p} - \mathbf{p}'$ is the transferred momentum, $\omega_q = sq$ is the phonon spectrum, and $s \sim 10^3$ m/s is the speed of sound. The above expression is valid in the phonon equipartition mode, i.e., when the speed of sound is well below the carrier thermal velocity. The detailed computation of phonon-induced resistivity $\rho_{e-ph}(T)$ in gapped graphene is beyond the scope of our paper. Yet, the anticipated dependence $\rho_{e-ph}(T)$ is the growing function of temperature, while electron-hole limited resistance decays with T, $\rho_{eh} \propto T^{-1}$. We can therefore expect the presence of a resistance minimum at some temperature T^*, which is

dictated by competition of electron-hole and electron-phonon scattering.

Our study was devoted to the 2D systems with massive Dirac-type spectrum. Yet, we argue that the cancellation of the Arrhenius-type exponents in the T dependence of ρ_{eh} is a general phenomenon which relies only on the Boltzmann statistics of electrons and holes at $E_g \gg kT$ and pair interactions between them. The subleading power-law factor in the T-dependent resistivity can depend on the particular form of the low-energy electron-hole Hamiltonian. It is not guaranteed that $\rho_{eh} \propto E_g/kT$ would hold for a massive Kane-type spectrum or for a tight-binding spectrum of bilayer graphene. The establishment of a power-law factor in these materials requires a separate consideration. A different situation also emerges in semimetals with overlapping conduction and valence bands, where CNP is achieved for a degenerate electron-hole system. Such a situation is realized in HgTe quantum wells above the critical thickness, where e-h scattering-limited resistivity scales as T^2 [35,36]. Scattering between degenerate electrons and degenerate holes can also be realized in drag experiments [14] and in 2D semiconductors with interband population inversion [34].

All the above discussion concerned the resistivity of gapped graphene exactly at the charge neutrality point. Away from the CNP, the electron-hole collisions make a minor contribution to the resistivity due to the effect of Coulomb drag [18,37]. More precisely, the majority carriers tend to drag the minority ones in the same direction, in spite of the opposite charges. The codirectional motion of electrons and holes reduces the strength of their mutual scattering. One may speculate that e-h scattering tends to nullify its own magnitude even for small density imbalance. An estimate of this imbalance can be obtained from the two-fluid hydrodynamic model [38] and reads as $\delta n/n_T \gtrsim \tau_{eh}/\tau_{ei}$. Definitely, a similar estimate could be obtained from a variational method using two different variational parameters τ_e and τ_h. We refrain from these lengthy calculations due to the expected minor effect of e-h collisions away from the CNP.

Potential extensions of this work lie in the field of thermoelectric coefficients of gapped graphene in the electron-hole collision regime. The interest to thermoelectricity in such a system stems from (1) enhancement of the Seebeck coefficient with gap induction even for impurity- and phonon-limited scattering and (2) further enhancement of thermopower and reduction in thermal conduction in the hydrodynamic regime [39,40]. The combination of these factors can make clean gapped graphene a very strong candidate for thermoelectric photodetection [41].

APPENDIX A: RESOLVING THE ENERGY CONSTRAINT FOR CARRIER-CARRIER SCATTERING

Equations for the scattering rates (17) and (18) are not yet suitable for numerical evaluation until the energy constraint given by the delta function is resolved. To achieve this, we introduce the extra transferred energy variable ω:

$$\delta(\varepsilon_{\mathbf{p}} + \varepsilon_{\mathbf{k}} - \varepsilon_{\mathbf{p}'} - \varepsilon_{\mathbf{k}'})$$
$$= \int d\omega\, \delta(\omega - \varepsilon_{\mathbf{p}} + \varepsilon_{\mathbf{p-q}})\delta(\omega - \varepsilon_{\mathbf{k+q}} + \varepsilon_{\mathbf{k}}). \quad \text{(A1)}$$

The expressions for C_{ee} and C_{eh} are factorized into the integrals of the general form

$$I(p, q, \omega) = \int d^2\mathbf{p}\, F(p, q, \theta_{\mathbf{pq}})\delta(\omega - \varepsilon_{\mathbf{p}} + \varepsilon_{\mathbf{p-q}}), \quad \text{(A2)}$$

where $F(p, q, \theta_{\mathbf{pq}})$ is some smooth function of absolute values of momenta p and q and the angle between them $\theta_{\mathbf{pq}}$.

We now integrate over the angle $\theta_{\mathbf{pq}}$. To achieve this, we perform a sequence of transformations:

$$\delta(\varepsilon_{\mathbf{p-q}} - \varepsilon_{\mathbf{p}} + \omega)$$
$$= (\varepsilon_{\mathbf{p-q}} + \varepsilon_{\mathbf{p}} - \omega)\delta\big[\varepsilon_{\mathbf{p-q}}^2 - (\varepsilon_{\mathbf{p}} - \omega)^2\big]$$
$$= 2(\varepsilon_{\mathbf{p}} - \omega)\delta\big[\varepsilon_{\mathbf{p}}^2 - 2pqv_0^2\cos\theta_{\mathbf{pq}} + q^2v_0^2 - (\varepsilon_p - \omega)^2\big]. \quad \text{(A3)}$$

The energy constraint is fulfilled at scattering angle θ^* given by

$$\theta^* = \arccos\left(\frac{\varepsilon_{\mathbf{p}}^2 + q^2v_0^2 - (\varepsilon_{\mathbf{p}} - \omega)^2}{2pqv_0^2}\right). \quad \text{(A4)}$$

Integration over the angle is now straightforward and results in

$$I(p, q, \omega) = 2\int \frac{p\,dp}{2pqv_0^2}\frac{2(\varepsilon_{\mathbf{p}} - \omega)}{\sin\theta^*}F(p, q, \theta^*). \quad \text{(A5)}$$

The factor of two before the whole expression comes from two scattering possibilities by angles $\pm\theta^*$.

APPENDIX B: RESISTIVITY AT LARGE BAND GAPS

Throughout this section, we work in the units $\hbar = k = v_0 = 1$. The resistivity of gapped graphene at $E_g \gg T$ is limited by normal electron-hole scattering. The annihilation-type process can be neglected due to its small matrix element, while electron-electron scattering can be neglected due to the approximate conservation of current if carriers reside at the parabolic part of the spectrum. The contribution of normal e-h scattering to average collision rate C, which we denote by C_{eh}^{++}, can be presented in the form [37,42]

$$C_{eh}^{++} = \frac{e^2\pi^2}{T}\int q\,dq\,d\omega|V(q)|^2 n_\omega[1 + n_\omega]$$
$$\times [\mathrm{Im}\Pi_0\mathrm{Im}\Pi_2 + \mathrm{Im}\boldsymbol{\Pi}_1\mathrm{Im}\boldsymbol{\Pi}_1], \quad \text{(B1)}$$

where $n_\omega = [e^{\omega/T} - 1]^{-1}$ are the Bose functions, and the "generalized polarizabilities" $\Pi_n(q, \omega)$ are defined by

$$\Pi_n(\mathbf{q}, \omega) = N\sum_{\mathbf{p}}\frac{f_0(\varepsilon_p) - f_0(\varepsilon_{p-q})}{\varepsilon_p - \varepsilon_{p-q} - \hbar\omega + i\delta}$$
$$\times |M_{\mathbf{p,p-q}}^{++}|^2(\mathbf{v}_{\mathbf{p}} - \mathbf{v}_{\mathbf{p-q}})^n. \quad \text{(B2)}$$

Representation (B1) is achieved by introducing an extra energy variable ω with the aid of (A1) and developing the square of four particle velocities:

$$[\mathbf{v_p} - \mathbf{v_k} - \mathbf{v_{p-q}} + \mathbf{v_{k+q}}]^2 = (\mathbf{v_p} - \mathbf{v_{p-q}})^2 + (\mathbf{v_k} - \mathbf{v_{k+q}})^2 - 2(\mathbf{v_p} - \mathbf{v_{p-q}})(\mathbf{v_k} - \mathbf{v_{k+q}}). \tag{B3}$$

Evaluation of the imaginary part of the polarizability is achieved with the Sokhotski rule

$$\text{Im}\Pi_0(\mathbf{q}, \omega) = -\pi N \sum_{\mathbf{p}} [f_0(\varepsilon_{\mathbf{p}}) - f_0(\varepsilon_{\mathbf{p-q}})]\delta[\varepsilon_{\mathbf{p}} - \varepsilon_{\mathbf{p-q}} - \omega]|M^{++}_{\mathbf{p,p-q}}|^2. \tag{B4}$$

The angular integration is performed with the aid of the delta function, which results in

$$\text{Im}\Pi_0(\mathbf{q}, \omega) = -\frac{N}{2\pi} \frac{1}{\sqrt{q^2 - \omega^2}} \int_{E_{\min}}^{\infty} d\varepsilon \left[f_0\left(\varepsilon + \frac{\omega}{2}\right) - f_0\left(\varepsilon - \frac{\omega}{2}\right) \right] \frac{\varepsilon^2 - \frac{q^2}{4}}{\sqrt{\varepsilon^2 - E_{\min}^2}}. \tag{B5}$$

The minimum carrier energy at which the quantum $(\mathbf{q}, \omega)$ can be absorbed is denoted by $E_{\min}$:

$$E_{\min} = \frac{q}{2}\sqrt{1 + \frac{E_g^2}{q^2 - \omega^2}}. \tag{B6}$$

Further integration over energies can be performed in the Boltzmann limit $E_g \gg T$. All slowly varying functions of energy ε can be evaluated at $\varepsilon = E_{\min}$, while the remainder is evaluated exactly:

$$\text{Im}\Pi_0(\mathbf{q}, \omega) = -\frac{\pi N}{(2\pi)^2} \frac{q^2 \sinh\left(\frac{\beta\omega}{2}\right)}{\sqrt{q^2 - \omega^2}} \sqrt{\pi}(B^2 - 1)\frac{e^{-\beta B q/2}}{\sqrt{\beta B q}}, \tag{B7}$$

where we have introduced the inverse temperature $\beta = T^{-1}$ and the dimensionless parameters

$$B(q, \omega) = \sqrt{1 + \frac{E_g^2}{q^2 - \omega^2}}, \quad l(q, \omega) = \frac{\omega}{q}. \tag{B8}$$

Similar steps can be done to evaluate $\text{Im}\Pi_{1,2}$ in the Boltzmann limit, which results in

$$\text{Im}\mathbf{\Pi}_1 = 2\pi \frac{N}{(2\pi)^2} \sinh\left(\frac{\beta\omega}{2}\right) \sqrt{q^2 - \omega^2} B\sqrt{\pi} \frac{B^2 - 1}{B^2 - l^2} \frac{e^{-\beta B q/2}}{\sqrt{\beta B q}} \frac{\mathbf{q}}{q}, \tag{B9}$$

$$\text{Im}\Pi_2 = 4\pi \frac{N}{(2\pi)^2} \sinh\left(\frac{\beta\omega}{2}\right) \sqrt{q^2 - \omega^2} B^2 \sqrt{\pi} \frac{B^2 - 1}{B^2 - l^2} \frac{1 - l^2}{B^2 - l^2} \frac{e^{-\beta B q/2}}{\sqrt{\beta B q}}. \tag{B10}$$

Considerable cancellations appear after collecting the expressions (B7)–(B10) into C_{eh}^{++}:

$$C_{eh}^{++} = \frac{\pi^3 N^2 e^2 \alpha_c^2}{8} \int dq\, d\omega \, \exp[-\beta E_g q B(q, \omega)] \frac{q^2 B(q, \omega)(q^2 - \omega^2)}{\left[q^2 + \frac{(q^2 - \omega^2)^2}{E_g^2}\right]^2}, \tag{B11}$$

where q and ω were normalized to the band gap E_g.

Let us inspect the function under the exponent $f(q) = qB(q, \omega)$. Considered as a function of q, it has a minimum value $f_{\min} = 1 + \omega$. Instead of q, we pass to the new variable

$$\tau = qB(q, \omega). \tag{B12}$$

The dimensionless integral in the expression for C_{eh}^{++} is now recast in the form

$$I \equiv \int dq\, d\omega \, \exp[-\beta E_g q B(q, \omega)] \frac{q^2 B(q, \omega)(q^2 - \omega^2)}{\left[q^2 + \frac{(q^2 - \omega^2)^2}{E_g^2}\right]^2} = 2\int_0^{\infty} d\omega \int_{1+\omega}^{\infty} d\tau \frac{\tau^2}{(\tau^2 - \omega^2)^2} \frac{e^{-\beta E_g \tau}}{\sqrt{(\tau^2 - \omega^2 - 1)^2 - 4\omega^2}}. \tag{B13}$$

Integrating over τ, we again proceed with the steepest descent method, i.e., we set $\tau = 1 + \omega$ in all smooth functions under the integration sign. This results in

$$I \approx \frac{(\beta E_g)^2}{2} \int_0^{\infty} d\omega \frac{(1 + \omega)^2}{[(1 + \omega)^2 - \omega^2]^2} \frac{1}{2\sqrt{\omega + 1}} \int_{1+\omega}^{\infty} d\tau \frac{e^{-\beta E_g \tau}}{\sqrt{\tau^2 - (1 + \omega)^2}}$$

$$= \frac{(\beta E_g)^2}{4} e^{-\beta E_g} \int_0^{\infty} d\omega \frac{(\omega + 1)^{3/2}}{(1 + 2\omega)^2} K_0(\omega \beta E_g) \approx \frac{\pi \beta E_g}{8} e^{-\beta E_g}. \tag{B14}$$

Hence

$$C_{eh}^{++} = \frac{N^2 e^2 \alpha^2}{8} (\beta E_g) \frac{\pi}{8} e^{-\beta E_g}. \qquad (B15)$$

Substituting C and D in the Boltzmann limit [Eqs. (B15) and (15)] into the general expression for the conductivity (13), we find the linear-in-T scaling of conductivity (21).

[1] K. S. Novoselov, A. K. Geim, S. V. Morozov, D. Jiang, M. I. Katsnelson, I. V. Grigorieva, S. V. Dubonos, and A. A. Firsov, Two-dimensional gas of massless Dirac fermions in graphene, Nature (London) **438**, 197 (2005).

[2] Y.-W. Tan, Y. Zhang, K. Bolotin, Y. Zhao, S. Adam, E. H. Hwang, S. Das Sarma, H. L. Stormer, and P. Kim, Measurement of scattering rate and minimum conductivity in graphene, Phys. Rev. Lett. **99**, 246803 (2007).

[3] K. I. Bolotin, K. J. Sikes, J. Hone, H. L. Stormer, and P. Kim, Temperature-dependent transport in suspended graphene, Phys. Rev. Lett. **101**, 096802 (2008).

[4] I. F. Herbut, V. Juricic, and O. Vafek, Coulomb interaction, ripples, and the minimal conductivity of graphene, Phys. Rev. Lett. **100**, 046403 (2008).

[5] E. G. Mishchenko, Minimal conductivity in graphene: Interaction corrections and ultraviolet anomaly, Europhys. Lett. **83**, 17005 (2008).

[6] E. V. Gorbar, V. P. Gusynin, V. A. Miransky, and I. A. Shovkovy, Magnetic field driven metal-insulator phase transition in planar systems, Phys. Rev. B **66**, 045108 (2002).

[7] K. Ziegler, Minimal conductivity of graphene: Nonuniversal values from the Kubo formula, Phys. Rev. B **75**, 233407 (2007).

[8] J. Martin, N. Akerman, G. Ulbricht, T. Lohmann, J. H. Smet, K. von Klitzing, and A. Yacoby, Observation of electron-hole puddles in graphene using a scanning single-electron transistor, Nat. Phys. **4**, 144 (2008).

[9] S. Adam, E. H. Hwang, V. M. Galitski, and S. Das Sarma, A self-consistent theory for graphene transport, Proc. Natl. Acad. Sci. USA **104**, 18392 (2007).

[10] V. V. Cheianov, V. I. Fal'ko, B. L. Altshuler, and I. L. Aleiner, Random resistor network model of minimal conductivity in graphene, Phys. Rev. Lett. **99**, 176801 (2007).

[11] Y. Cao, A. Mishchenko, G. L. Yu, E. Khestanova, A. P. Rooney, E. Prestat, A. V. Kretinin, P. Blake, M. B. Shalom, C. Woods, J. Chapman, G. Balakrishnan, I. V. Grigorieva, K. S. Novoselov, B. A. Piot, M. Potemski, K. Watanabe, T. Taniguchi, S. J. Haigh, A. K. Geim *et al.*, Quality heterostructures from two-dimensional crystals unstable in air by their assembly in inert atmosphere, Nano Lett. **15**, 4914 (2015).

[12] Y. Nam, D.-K. Ki, D. Soler-Delgado, and A. F. Morpurgo, Electron-hole collision limited transport in charge-neutral bilayer graphene, Nat. Phys. **13**, 1207 (2017).

[13] A. I. Berdyugin, N. Xin, H. Gao, S. Slizovskiy, Z. Dong, S. Bhattacharjee, P. Kumaravadivel, S. Xu, L. A. Ponomarenko, M. Holwill, D. A. Bandurin, M. Kim, Y. Cao, M. T. Greenaway, K. S. Novoselov, I. V. Grigorieva, K. Watanabe, T. Taniguchi, V. I. Fal'ko, L. S. Levitov *et al.*, Out-of-equilibrium criticalities in graphene superlattices, Science **375**, 430 (2022).

[14] D. A. Bandurin, A. Principi, I. Y. Phinney, T. Taniguchi, K. Watanabe, and P. Jarillo-Herrero, Interlayer electron-hole friction in tunable twisted bilayer graphene semimetal, Phys. Rev. Lett. **129**, 206802 (2022).

[15] P. Gallagher, C.-S. Yang, T. Lyu, F. Tian, R. Kou, H. Zhang, K. Watanabe, T. Taniguchi, and F. Wang, Quantum-critical conductivity of the Dirac fluid in graphene, Science **364**, 158 (2019).

[16] J. Crossno, J. K. Shi, K. Wang, X. Liu, A. Harzheim, A. Lucas, S. Sachdev, P. Kim, T. Taniguchi, K. Watanabe, T. A. Ohki, and K. C. Fong, Observation of the Dirac fluid and the breakdown of the Wiedemann-Franz law in graphene, Science **351**, 1058 (2016).

[17] W. Zhao, S. Wang, S. Chen, Z. Zhang, K. Watanabe, T. Taniguchi, A. Zettl, and F. Wang, Observation of hydrodynamic plasmons and energy waves in graphene, Nature (London) **614**, 688 (2023).

[18] V. Vyurkov and V. Ryzhii, Effect of the Coulomb scattering on graphene conductivity, JETP Lett. **88**, 322 (2008).

[19] A. B. Kashuba, Conductivity of defectless graphene, Phys. Rev. B **78**, 085415 (2008).

[20] L. Fritz, J. Schmalian, M. Müller, and S. Sachdev, Quantum critical transport in clean graphene, Phys. Rev. B **78**, 085416 (2008).

[21] J. Jung, A. M. DaSilva, A. H. MacDonald, and S. Adam, Origin of band gaps in graphene on hexagonal boron nitride, Nat. Commun. **6**, 6308 (2015).

[22] E. McCann, D. S. L. Abergel, and V. I. Fal'ko, The low energy electronic band structure of bilayer graphene, Eur. Phys. J.: Spec. Top. **148**, 91 (2007).

[23] Y. Zhang, T. T. Tang, C. Girit, Z. Hao, M. C. Martin, A. Zettl, M. F. Crommie, Y. R. Shen, and F. Wang, Direct observation of a widely tunable bandgap in bilayer graphene, Nature (London) **459**, 820 (2009).

[24] M. König, S. Wiedmann, C. Brüne, A. Roth, H. Buhmann, L. W. Molenkamp, X.-L. Qi, and S.-C. Zhang, Quantum spin hall insulator state in hgte quantum wells, Science **318**, 766 (2007).

[25] M. Marcinkiewicz, S. Ruffenach, S. S. Krishtopenko, A. M. Kadykov, C. Consejo, D. B. But, W. Desrat, W. Knap, J. Torres, A. V. Ikonnikov, K. E. Spirin, S. V. Morozov, V. I. Gavrilenko, N. N. Mikhailov, S. A. Dvoretskii, and F. Teppe, Temperature-driven single-valley Dirac fermions in HgTe quantum wells, Phys. Rev. B **96**, 035405 (2017).

[26] M. Zarenia, S. Adam, and G. Vignale, Temperature collapse of the electric conductivity in bilayer graphene, Phys. Rev. Res. **2**, 023391 (2020).

[27] C. Tan, D. Y. H. Ho, L. Wang, J. I. A. Li, I. Yudhistira, D. A. Rhodes, T. Taniguchi, K. Watanabe, K. Shepard, P. L. McEuen, C. R. Dean, S. Adam, and J. Hone, Dissipation-enabled hydrodynamic conductivity in a tunable bandgap semiconductor, Sci. Adv. **8**, eabi8481 (2022).

[28] L. Landau, The kinetic equation in the case of Coulomb interaction, Phys. Z. Sowjetunion **10**, 154 (1936).

[29] M. Combescot and R. Combescot, Conductivity relaxation time due to electron-hole collisions in optically excited semiconductors, Phys. Rev. B **35**, 7986 (1987).

[30] J. M. Ziman, *Electrons and Phonons: The Theory of Transport Phenomena in Solids* (Oxford University Press, Oxford, 2001).

[31] P. F. Maldague and C. A. Kukkonen, Electron-electron scattering and the electrical resistivity of metals, Phys. Rev. B **19**, 6172 (1979).

[32] K. Takahashi, H. Matsuura, H. Maebashi, and M. Ogata, Thermoelectric properties in semimetals with inelastic electron-hole scattering, Phys. Rev. B **107**, 115158 (2023).

[33] Following Ziman [43], it is possible to show that $\mathcal{Q}[\Phi] = \frac{1}{2}\frac{\partial S_{coll}}{\partial t} - \frac{\partial S_{field}}{\partial t}$; here $\partial S_{coll}/\partial t$ and $\partial S_{field}/\partial t$ are the entropy generation rate during collisions and entropy removal rate by the electric field. In a steady state $\frac{\partial S_{field}}{\partial t} = \frac{\partial S_{coll}}{\partial t}$ and thus $\mathcal{Q}[\Phi] = -\frac{1}{2}\frac{\partial S_{coll}}{\partial t}$. Minimum of $\mathcal{Q}[\Phi]$ thus corresponds to maximization of entropy generation rate by collisions.

[34] D. Svintsov, V. Ryzhii, A. Satou, T. Otsuji, and V. Vyurkov, Carrier-carrier scattering and negative dynamic conductivity in pumped graphene, Opt. Express **22**, 19873 (2014).

[35] Z. D. Kvon, E. B. Olshanetsky, E. G. Novik, D. A. Kozlov, N. N. Mikhailov, I. O. Parm, and S. A. Dvoretsky, Two-dimensional electron-hole system in HgTe-based quantum wells with surface orientation (112), Phys. Rev. B **83**, 193304 (2011).

[36] M. V. Entin, L. I. Magarill, E. B. Olshanetsky, Z. D. Kvon, N. N. Mikhailov, and S. A. Dvoretsky, The effect of electron-hole scattering on transport properties of a 2D semimetal in the HgTe quantum well, J. Exp. Theor. Phys. **117**, 933 (2013).

[37] M. Zarenia, A. Principi, and G. Vignale, Disorder-enabled hydrodynamics of charge and heat transport in monolayer graphene, 2D Mater. **6**, 035024 (2019).

[38] D. Svintsov, V. Vyurkov, S. Yurchenko, T. Otsuji, and V. Ryzhii, Hydrodynamic model for electron-hole plasma in graphene, J. Appl. Phys. **111**, 083715 (2012).

[39] T. I. Andersen, T. B. Smith, and A. Principi, Enhanced photoenergy harvesting and extreme Thomson effect in hydrodynamic electronic systems, Phys. Rev. Lett. **122**, 166802 (2019).

[40] A. Principi and G. Vignale, Violation of the Wiedemann-Franz law in hydrodynamic electron liquids, Phys. Rev. Lett. **115**, 056603 (2015).

[41] E. Titova, D. Mylnikov, M. Kashchenko, I. Safonov, S. Zhukov, K. Dzhikirba, K. S. Novoselov, D. A. Bandurin, G. Alymov, and D. Svintsov, Ultralow-noise terahertz detection by p-n junctions in gapped bilayer graphene, ACS Nano **17**, 8223 (2023).

[42] L. Zheng and A. H. MacDonald, Coulomb drag between disordered two-dimensional electron-gas layers, Phys. Rev. B **48**, 8203 (1993).

[43] J. M. Ziman, The general variational principle of transport theory, Can. J. Phys. **34**, 1256 (1956).